Air-Coupled Piezoelectric Detection of Laser-Generated Ultrasound

David A. Hutchins, William M. D. Wright, Gordon Hayward, *Senior Member, IEEE,* and Anthony Gachagan

Abstract—**A pulsed laser has been used to generate ultrasonic transients in samples of metal and fiber-reinforced polymer composite material. These have been detected using an air-coupled piezoelectric transducer. It is demonstrated that such a transduction system can be used for longitudinal waves in bulk material, Rayleigh waves at solid surfaces and Lamb waves in thin plates.**

I. Introduction

THE USE OF PULSED LASERS for ultrasonic generation in solid materials has been of interest in recent years, particularly for nondestructive evaluation applications. The approach does not involve surface contact, and allows the source to be scanned over an object (which may be at high temperatures) with minimal surface contamination [1], [2]. It thus has a considerable advantage in some respects over the more conventional contacting piezoelectric transducers as an ultrasonic source.

There are several mechanisms whereby a laser pulse can be used to generate ultrasonic transients in both fluids and solids [1]. Common to all substances is the thermoelastic effect. Here, energy is absorbed from the laser pulse, and rapid thermal expansion occurs. Assuming that a change of state of the substance does not occur, this is likely to be the dominant mechanism. At a solid surface in particular, as this is the present case of interest, the stresses tend to be radial and parallel to the irradiated surface. The time history of the excitation is step-like, being the integral of that of the incident laser pulse. If the optical power density is increased, ablation of solid material can occur. Ablated material causes forces normal to the surface to exist, thus modifying the characteristics of the source and the radiated acoustic waves. A further mechanism of interest is that produced by a dielectric breakdown of air [3].

Pulsed lasers can generate both longitudinal and shear waves in a bulk solid material. With the source and receiver aligned on opposite sides of a parallel-sided solid sample, thermoelastic generation mechanisms lead to a predicted theoretical waveform with a large shear arrival. An ablative source leads to a much-enhanced longitudinal signal, where now the longitudinal displacement is pulse-like, with little of the ringing associated with more conventional sources. This is also the case with an air breakdown source. The laser can also be used as an efficient source of Rayleigh (surface) waves at a solid surface, and Lamb waves in a thin plate. The Rayleigh waves are bipolar in general, with a time duration which usually depends on the width of the source at the solid surface. Lamb wave propagation is more complicated, in that there are two families of Lamb mode (symmetric and antisymmetric), all of which are dispersive (i.e., their phase velocity is a function of frequency), and within which there are a series of orders.

A completely noncontacting ultrasonic system requires a suitable detector to be available, and several approaches have been described in the literature. The most common method is to use some form of optical device, based on either interferometry or laser beam deflection [4], [5]. This approach leads to an all-optical system which has many attractions [6], in that it can operate over a reasonable bandwidth at some distance from the sample. The principal disadvantage is that the detection surface must have a reasonably good surface finish, in terms of roughness, reflectivity and surface tilt, so that enough light is returned to the optical sensing arrangement.

If the surface is electrically conducting, then two other noncontact methods are available. The first of these, a capacitance transducer, can provide displacement waveforms over a wide bandwidth as a point measurement, with a reasonable sensitivity [7], [8]. Because of the small gap required, it is most useful as a calibration device, and is used as such in this paper. An alternative approach is to use an electromagnetic acoustic transducer (EMAT) [9], [10]. The main disadvantages of these devices are they both require an electrically conducting sample, and a stand-off gap of less than 1mm in most cases.

There has been recent interest in ultrasonic transducers that can operate in air at high frequencies, as these can be used at a much greater distance from the sample, and may be used to inspect nonconductive materials such as polymers and composites. There are basically two types of transducer: capacitance (or electrostatic) devices, and piezoelectric designs which are used in this work. The former type use a flexible metallized membrane, stretched over a roughened conducting backplate [11], [12]. The response of these devices is controlled by several factors, but one of the most important is the resonance of small air pockets trapped between the membrane and the backplate. Careful control of the surface finish of the backplate needs to be maintained, and to date such devices have been designed for operation up to approximately 2 MHz.

Piezoceramic transducers in their conventional form (i.e., for operation in liquids or at a solid interface) do not perform well

Manuscript received February 3, 1994; revised May 19, 1994; accepted June 1, 1994. This work was supported by the Science and Engineering Research Council (SERC), UK.

D. A. Hutchins and W. M. D. Wright are with the Department of Engineering, University of Warwick, Coventry, CV4 7AL, England.

G. Hayward and A. Gachagan are with the Department of Electronic and Electrical Engineering, University of Strathclyde, Glasgow G1 1XW, Scotland.

IEEE Log Number 9405225.

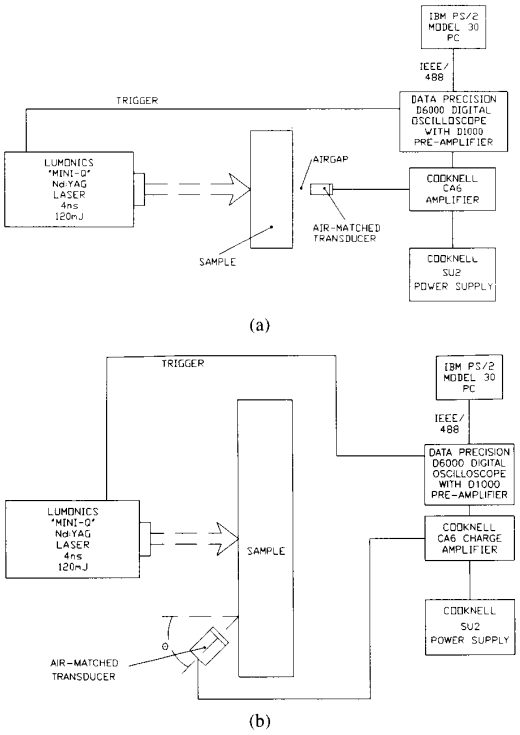

Fig. 1. Schematic diagrams ofthe apparatus used to collect noncontact ultrasonic waveforms for (a) longitudinal and shear waves and (b) Rayleigh and Lamb waves.

in air, due to the acoustic impedance mismatch between air and the piezoceramic element (usually lead zirconate titanate). Developments to overcome this constraint have involved the introduction of multiple matching layers [13] or the application of a radiating membrane [14] to facilitate the energy transfer into air. This work employs the 1–3 connectivity piezocomposite transducer [15, 16], comprising active piezoceramic and passive polymer phases providing a reduction in the acoustic impedance and an enhanced efficiency when compared with conventional piezoceramic. Detailed investigation by the authors into the application of 1–3 connectivity piezocomposite transducers to airborne ultrasound [17] has enabled the construction of the detectors utilized in this work, as described in the next section.

The present paper investigates a new noncontact transducer combination, that uses an air-coupled piezoelectric detector in conjunction with pulsed laser generation. In the following, the new hybrid system is described, and results given of ultrasonic waveforms in both metals and fiber-reinforced composites. It will be shown that this combination works well for a range of ultrasonic modes, including longitudinal, Rayleigh and Lamb waves.

II. Apparatus and Experiment

A schematic diagram of the apparatus used to perform longitudinal wave experiments is shown in Fig. 1(a). The laser source was a "mini-Q" Q-switched Nd:YAG laser, which provided single pulses of 4 ns duration at a maximum energy

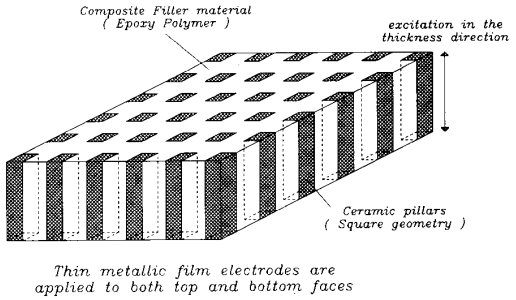

Fig. 2. Ceramic-epoxy composite structure for 1–3 connectivity transducers.

of 120 mJ per pulse, at an optical wavelength of 1.06 μm. These were directed onto the sample using a dielectric mirror. The beam diameter could be altered using an adjustable iris aperture, and focused using lenses of various types (conventional and cylindrical) with the desired focal length. In this way, the size and shape of the incident laser beam at the surface could be changed, with a concurrent adjustment of the incident optical power density.

In the present measurements, the samples were in the form of parallel-sided plates of either aluminium or various types of fiber-reinforced polymer composite. In a typical arrangement, Fig. 1(a), the laser pulse created an acoustic source on one side of the plate. Ultrasonic transients travelled through the sample, and hence into the air beyond having passed across the sample/air interface. Note that there would be a large reflection coefficient (α_r) at this interface, given by the expression

$$\alpha_r = \left[\frac{(Z_2 - Z_1)}{(Z_2 + Z_1)}\right]^2 \tag{1}$$

This is because Z_1 and Z_2 for the solid sample and air, respectively, are very different. Nevertheless, there would still be some transmission into the air beyond, in the form of a longitudinal wave which would travel to the air-coupled piezoelectric detector, which was carefully aligned with the source. Signals from the detector were amplified using a Cooknell CA6 charge amplifier, and digitised using a Data Precision Data 6000 digital oscilloscope. The oscilloscope was triggered using a synchronization signal from the Pockels Cell of the pulsed laser. Recorded waveforms were transferred to an IBM PS/2 computer over an IEEE interface for subsequent storage and analysis.

A slightly modified arrangement was used for Rayleigh waves on the surface of thick samples and Lamb waves in thin plates, as shown in Fig. 1(b). Here, the air-coupled piezoelectric detector was displaced along the sample surface, and the sample rotated to vary the angle θ between the transducer and the sample surface. The detection of these modes relies on the fact that they are "leaky", i.e., they radiate energy out into the surrounding fluid, in this case air. The energy is emitted at a characteristic angle (θ_c), which depends on the wave propagation velocity in both the sample (c_w) and air (c_{air}). The angle (θ_c) is given by

$$\theta_c = \sin^{-1}\left[\frac{c_{\text{air}}}{c_w}\right] \tag{2}$$

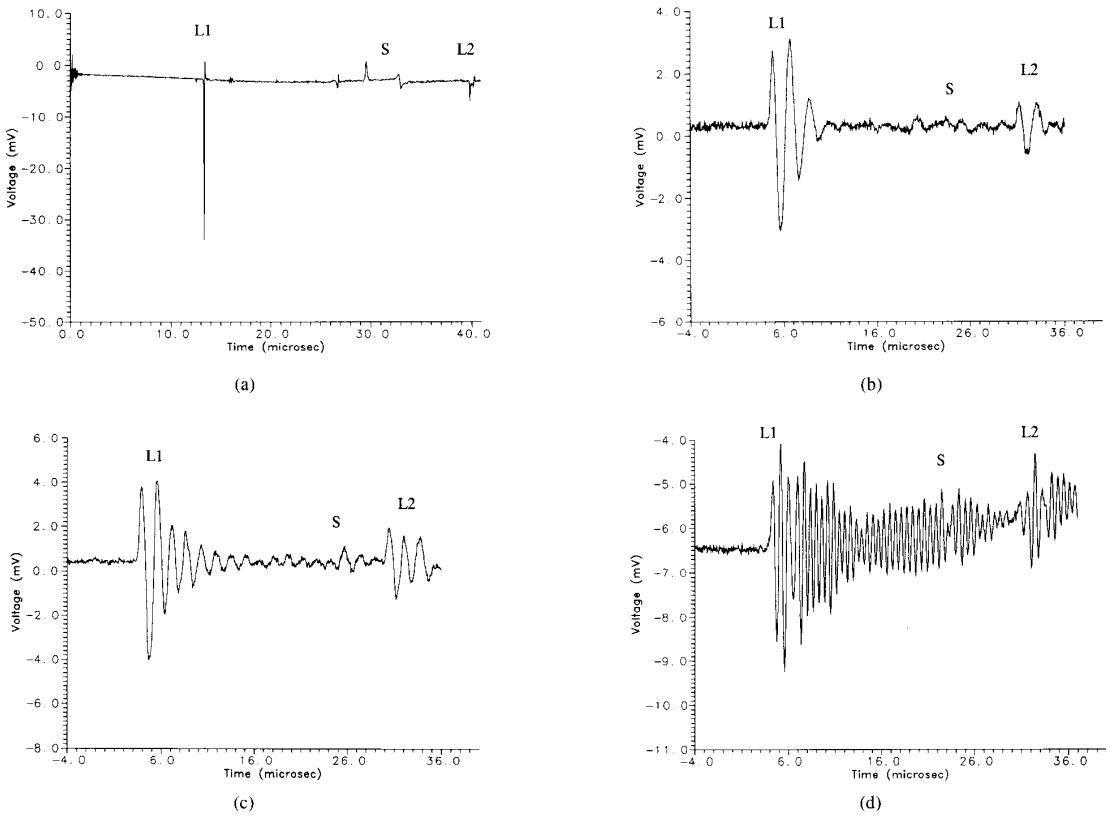

Fig. 3. Waveforms detected in an 86 mm thick aluminium block, using the experimental arrangement of Fig. 1(a). The detectors were (a) the capacitance transducer, (b) the undamped lower frequency air-coupled device, (c) the damped device, and (d) the higher frequency transducer.

TABLE I

	Transducer #1	Transducer #2	Transducer #3
volume fraction (%)	40	40	40
f_e (kHz)	525	541	1720
f_m (kHz)	643	656	1985
k_t	0.617	0.605	0.538
Z_{ml} (MRayl)	1.0	1.0	1.0
matching layer thickness(mm)	0.4	0.4	0.13
Z_{bb} (MRayl)	8.0	none	none
backing block length (mm)	40	/	/

For a Rayleigh wave, c_w is fixed, and hence, so is θ_c. Lamb waves are dispersive, however, and the phase velocity will depend on the frequency and Lamb mode of interest, and the thickness of the plate. Hence, the optimum value of θ_c for a given Lamb mode and sample will change with frequency. To state this another way, fixing the detector at some angle θ_c will naturally select frequencies of particular Lamb modes that radiate at that particular angle. Note that in the case of Lamb wave propagation, the receiver could be placed on either face of the plate-like samples, as both surfaces are coupled in Lamb wave motion.

The piezoelectric detectors were based on a 1–3 connectivity composite, and a schematic diagram of such a structure is presented in Fig. 2. These devices were manufactured by utilising the standard slice and fill technique [15] producing a transducer which comprises a matrix of piezoceramic pillars embedded in a polymer filler material. Careful design of constituent materials together with the distribution and geometry of the ceramic pillars enable the adjustment of the acoustic impedance, bandwidth and thickness mode coupling coefficient for the application under consideration. This was achieved through the application of computer simulation models, where finite element modeling [15] and a linear systems approach [16] have both been employed. The introduction of an intermediate matching layer, secured to the front face of the transducer, and/or a backing block, attached to the rear face of the device, influences both the sensitivity and bandwidth of the device. Again, theoretical modeling was used to obtain a satisfactory compromise between ease of manufacture, sensitivity and frequency response.

Three prototype transducers were manufactured, with each device comprising square PZT-5A piezoceramic pillars, embedded in CIBA-GEIGY CY1301/HY1300 hard setting epoxy. Each transducer was 30 mm in diameter and housed in an electrically screened metal casing. Additional details of the transducer characteristics are provided in Table I, where k_t is the fundamental thickness mode coupling coefficient, f_e and f_m are the frequencies of electrical (impedance minimum) and mechanical (impedance maximum) resonance, Z_{ml} is the acoustic impedance of the matching layer and Z_{bb} is the acoustic impedance of the backing material. The matching

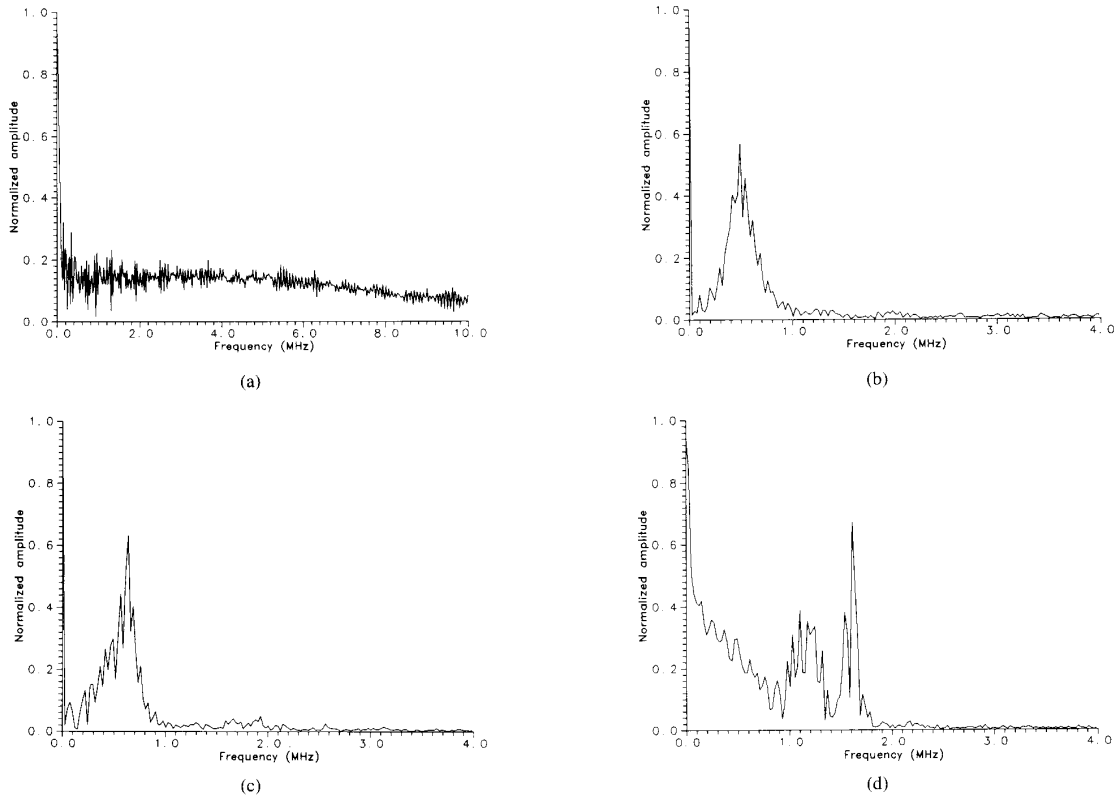

Fig. 4. Frequency spectra of a longitudinal arrival from each of the waveforms in Fig. 3.

layer material utilized was RTV Silicone Rubber, at a quarter wavelength of the transducer fundamental frequency, with Tungsten loaded hard setting epoxy employed as a damped backing medium.

To provide calibration waveforms against which to compare the outputs of the air-coupled devices, a capacitance transducer was used at some metal surfaces to detect ultrasonic displacements generated by the laser source. This consisted of an insulated ball-bearing, of 15 mm diameter, to which a 100 V dc bias was applied. It was placed within a few μm of the surface, using a thin polymer sheet to stop grounding of the electrode and to increase the dielectric constant in the gap. Ultrasonic displacements caused the gap between the electrode and the surface to change, causing a change in charge which was fed into a charge amplifier to give a voltage output. The present device had a flat response over a 10 MHz bandwidth. Note that the curved nature of the ball-bearing electrode meant that alignment was not a crucial factor in the device performance-only the gap was a factor.

III. Results and Discussion

A. System Response

The first experiments were designed to investigate the response of a combined laser generation/air-coupled detector system, using the arrangements of Fig. 1 and aluminium samples of various sizes. Three air-coupled detectors were used and compared in this initial study. As mentioned above, two of the devices had a nominal centre frequency of around 650 kHz, one being damped and the other being without any form of backing layer. An additional undamped detector was also used, this being designed to operate at a frequency of approximately 2 MHz.

To investigate longitudinal and shear wave generation, the transducers were positioned in turn at the far side of a 86 mm thick aluminium calibration block, and the pulsed Nd:YAG laser was focused to a 2 mm diameter spot to generate ultrasonic signals by both thermoelastic generation and by evaporation of a thin oil coating. This gave increased signal amplitude similar to an ablative source, but without the associated surface damage to the sample. The resulting waveforms were then detected by both the air-coupled devices with an airgap of 10 mm, and a capacitance transducer in contact with the sample. The latter was used here as a calibration device against which to compare signals detected by the air-coupled devices.

Fig. 3(a) shows the waveform detected by the capacitance transducer for a liquid evaporation source, this detector producing a broad bandwidth output without the resonances associated with piezoelectric devices. Note the characteristics mentioned earlier, namely a longitudinal signal $L1$ and its echo $L2$, generated by the evaporation source which is almost δ-function in time. The shear arrival S was a small step feature, at twice the propagation delay. The waveform of Fig. 3(a) may be compared to those derived from the air-coupled devices for

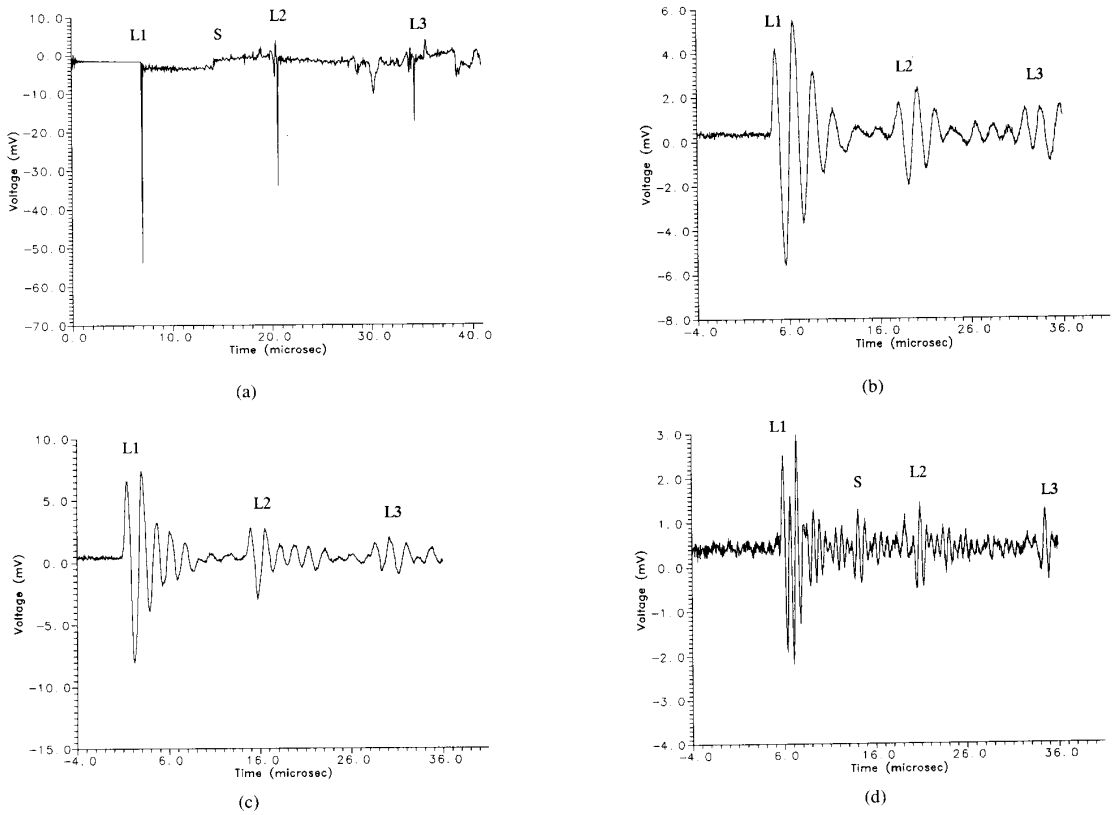

Fig. 5. Waveforms detected in an 44 mm thick aluminium plate, using the experimental arrangement of Fig. 1(a). The detectors were (a) the capacitance transducer, (b) the undamped lower frequency air-coupled device, (c) the damped device, and (d) the higher frequency transducer.

the same generation conditions, as shown in Figs. 3 (b)–(d), where the waveforms are again dominated by the longitudinal signals $L1$ and $L2$. Note that the time delay introduced by propagation through the air gap between the sample and the detector has been removed for presentation purposes. The response of each device can be illustrated further by obtaining the frequency spectrum of the first longitudinal arrival $L1$ only, using a Fast Fourier Transform (FFT). The results are shown in Fig. 4. The capacitance device [Fig. 4(a)] demonstrates the broad bandwidth response expected, whereas Figs. 4(b) and (c) demonstrate that the lower frequency air-coupled devices have a peak response in the 600–700 kHz range, but with a better response as expected for the damped transducer. The corresponding spectrum for the higher frequency device [Fig. 4(d)] indicates operation at frequencies in the 1–2 MHz region.

B. Waveforms and Deconvolution in Aluminium Plates

Waveforms were now recorded with the air-coupled detectors at selected distances of the detector from aluminium samples of different thickness. Consider first the capacitance transducer waveform in a sample in the form of a 44 mm thick plate, as shown in Fig. 5(a). There are several interesting features. There is a clear first longitudinal arrival $L1$, which has traveled through the aluminium block and directly to the detector. This is followed by the step like shear arrival S, and then multiple reflections $L2$ and $L3$, within the metal sample. Waveforms detected by the three piezoelectric devices are shown in Figs. 5(b)–(d). Note that multiple reflections within the air gap between sample and detector have too long a propagation delay to appear on the waveform. The undamped lower frequency device [Fig. 5(b)] shows the multiple longitudinal reflections in the sample clearly, with some evidence of shear mode detection, although the latter mode is enhanced in the waveforms from the other transducers [Figs. 5(c) and (d)]. It is not possible to resolve the shear wave arrival S, except in Fig. 5(d). Note that the time per division in these figures is the same, although the absolute time delay differs due to propagation delays through the air to the detector. From such waveforms, it would be possible to extract information concerning either the sample thickness, or its longitudinal velocity (and possibly the shear velocity, and hence the elastic properties of the material).

Similar experiments were also performed in a thinner (19.8 mm thick) aluminium plate and the resulting waveforms are shown in Fig. 6. Note that now the multiple longitudinal echoes $L1$ to $L3$ are moved closer together in the capacitive transducer response, and tend to merge for the air-coupled devices with the more limited bandwidth. From such waveforms, it would not be possible to extract information concerning the material directly. To help overcome this, deconvolution

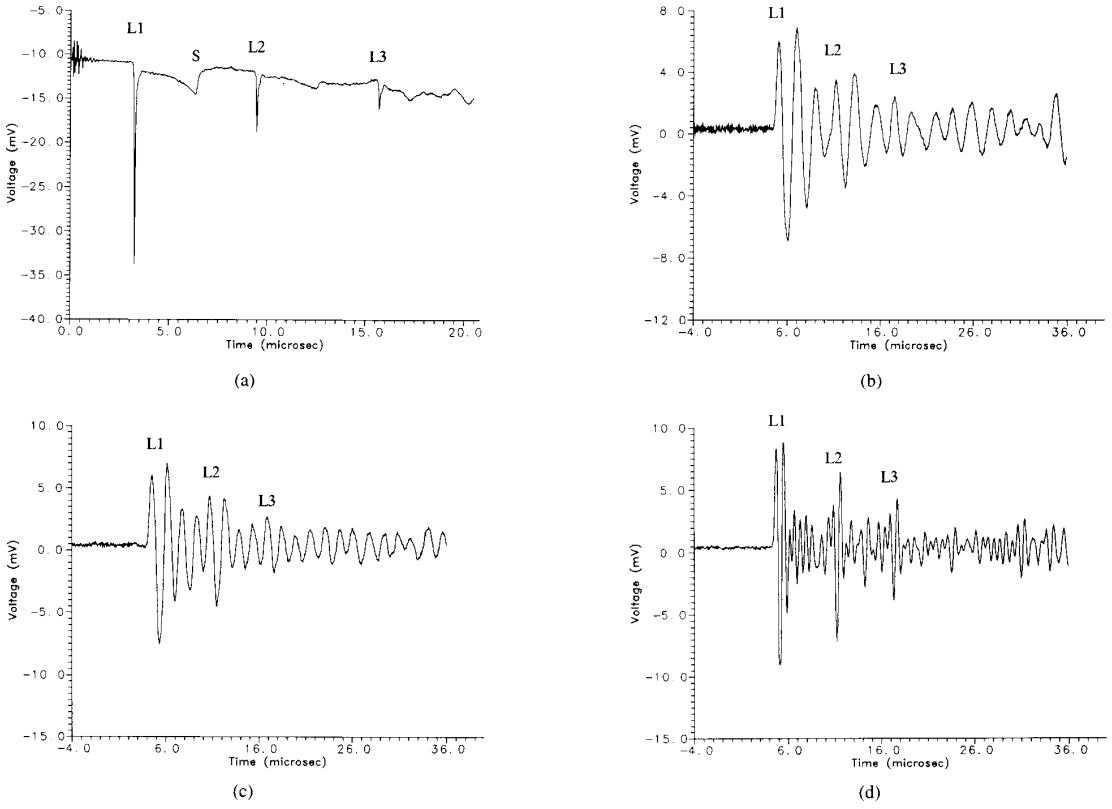

Fig. 6. Waveforms detected in an 19.8 mm thick aluminium plate, using the experimental arrangement of Fig. 1(a). The detectors were (a) the capacitance transducer, (b) the undamped lower frequency air-coupled device, (c) the damped device, and (d) the higher frequency transducer.

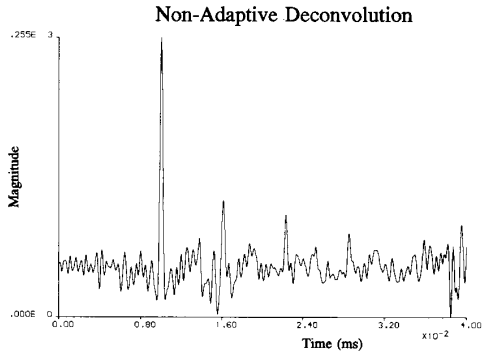

Fig. 7. Minimum entropy deconvolved result from signal in Fig. 6(d).

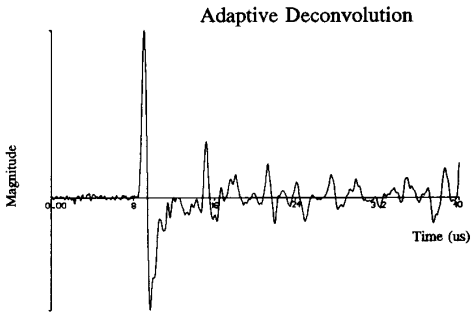

Fig. 8. MLMS deconvolved result from signal in Fig. 6(d).

techniques have been applied to the waveform, where adaptive [18] and nonadaptive [19], [20] deconvolution techniques were used in an effort to produce the desired pulse compression.

The adaptive approaches selected utilized an autoregressive model, which generates a signal estimate sequence and a weight (tapped delay filter coefficients) sequence to produce an error sequence, i.e., the deconvolved output. This technique permits the signal processing algorithms to follow the evolution of the waveform. The main disadvantage with the method is that the algorithm prefers minimum delay characteristics, which the waveform in question does not exhibit. Thus the resulting output have a suboptimal resolution capacity. The nonadaptive deconvolution techniques require the acquisition of a reference wavelet, which is the impulse response of the system. This reference wavelet can then be employed to form an inverse filter in a classical deconvolution approach or directly as in probabilistic deconvolution utilizing estimation techniques. Although the majority of these algorithms also require minimum delay characteristics, there are available a few algorithms that operate well on the mixed phase waveform detected by this hybrid system. For the waveform shown in Fig. 6(d) two deconvolved results are presented, one each for the adaptive and nonadaptive deconvolution techniques.

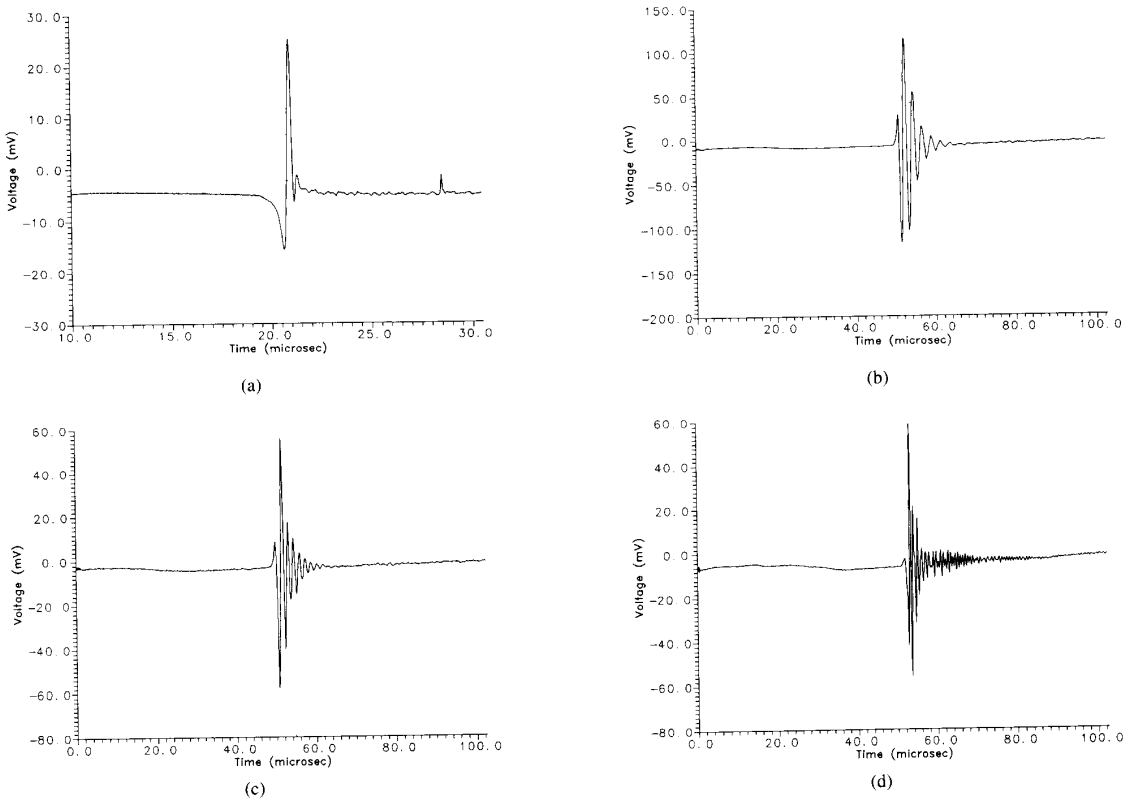

Fig. 9. Rayleigh waveforms in a thick aluminium block, using the configuration of Fig. 1(b). (a) is the capacitance transducer waveform, and (b)–(d) are those from the three air-coupled devices at an angle (θ_c) of 6°.

The nonadaptive approach is presented in Fig. 7, which depicts the deconvolved output from the Minimum Entropy algorithm [20]. This is an iterative algorithm, which is computationally excessive and consequently very slow. The algorithm has performed quite well, with excellent signal definition. The deconvolved output shows that the algorithm has decoded the first through transmitted pulse and three internal reflection pulses. The adaptive approach is presented in Fig. 8, where the modified least means squared algorithm, which is based on the Adaptive Line Enhancer configuration, has been employed [18]. The deconvolved result has extracted the first through transmitted pulse and two internal reflection pulses, but with reduced resolution when compared to the Minimum Entropy deconvolved result. In both deconvolved results shear wave mode conversions are present in between the reflected pulses, which could be interpreted as flaw characteristics in an NDE environment. However, given sufficient *a priori* information, it may be possible to remove such multiples by similar deconvolution procedures.

C. Rayleigh and Lamb Waves

These experiments used the configuration shown earlier in Fig. 1(b), with the laser-induced source and the air-coupled piezoelectric detector on the same side of a thick aluminium block. To optimize detection sensitivity of the energy radiated by the leaky Rayleigh or Lamb mode, the axis of the air-coupled detector was aligned at an adjustable angle θ from the normal through the surface of the sample. This angle would be set at the critical angle θ_c defined by (2) for the mode of interest (e.g., for Rayleigh waves in aluminium, with a velocity of 3100 ms^{-1}, θ_c would be approximately 6°). Waveforms were also detected at an aluminium surface using the capacitance transducer device described earlier.

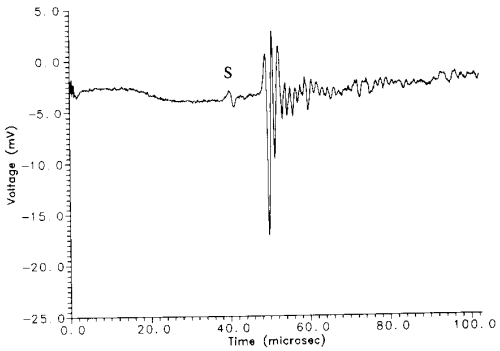

Fig. 10. Rayleigh waveform for the damped air-coupled detector at $\theta = 3°$.

An example of a typical Rayleigh waveform recorded using the capacitance transducer on an aluminium surface is shown in Fig. 9(a). Note again the lack of ringing in the signal. Waveforms derived from the three air-coupled piezoelectric

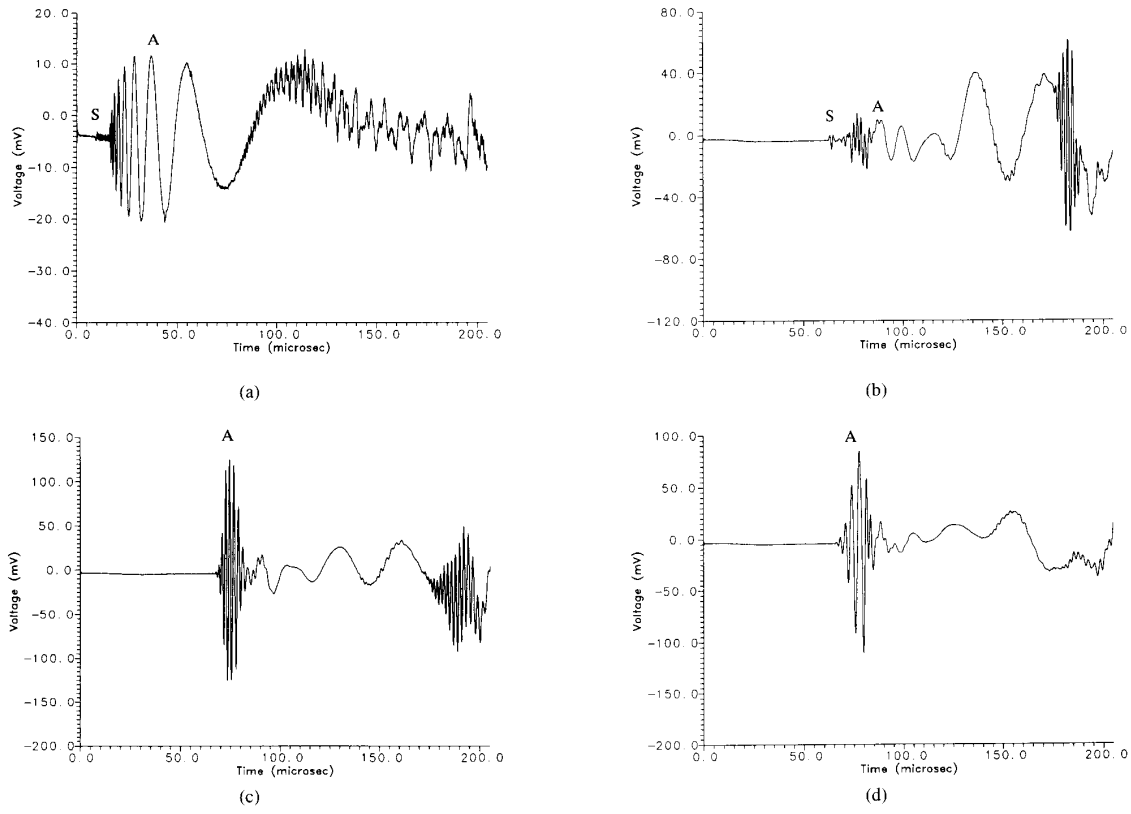

Fig. 11. Lamb waveforms in a 0.86 mm thick aluminium plate, as detected by (a) the capacitance transducer, and (b)–(d) the air-coupled piezoelectric devices.

detectors are presented in Figs. 9(b)–(d), with the detectors at the optimum angle (θ_c) of 6°. Clear Rayleigh signals were obtained, and it is evident that despite the large difference in acoustic impedance between the aluminium sample and air, enough energy was radiated into the air by the leaky Rayleigh wave to form a detectable signal. An interesting feature was observed, in that changing the angle to $\theta = 3°$ caused the features of the waveforms to change, with an additional signal S arriving before the main Rayleigh signal, the latter being of reduced amplitude. This is shown in Fig. 10. This small initial arrival S is due to the surface-skimming longitudinal wave, travelling parallel to the metal surface. One complication with this type of arrangement is that there is a direct air path to the receiver for air-borne acoustic transients generated at the source. In fact, this signal arrives *after* the leaky Rayleigh wave signal, due to the fact that the Rayleigh velocity is almost an order of magnitude greater than that of longitudinal waves in air, and hence does not appear on the present waveforms. It could be blocked off by an attenuating material if it caused a problem, but this was not necessary here.

As stated previously, the case of Lamb wave propagation is more complicated, in that dispersion causes the wave velocity to be a function of frequency, and hence the angle θ at which the detector is inclined would act as a form of selection for various modes and frequencies. For a particular frequency response of the detector, there is thus likely to be an optimum angle for the detection of a particular Lamb mode. Fig. 11(a) shows the time waveform detected by the capacitance transducer of Fig. 3 for Lamb waves generated by the laser in a 0.85 mm thick aluminium plate. The small high frequency initial signal S is the s_0 Lamb mode, and this is followed by the dispersive a_0 mode A, with lower frequencies (of higher amplitude) arriving later. The response of the air-coupled detectors is illustrated by the undamped lower frequency device at various angles (θ) of the detector and for a sample/receiver separation of 20 mm. At $\theta = 5°$ [Fig. 11(b)], detection of the s_0 mode is optimized, whereas at $\theta = 12°$, Fig. 11(c), the a_0 mode is detected as a clear signal. Finally, at $\theta = 17°$ [Fig. 11(d)], the a_0 is still detected, but at a lower frequency due to the increased angle θ to the surface. This is expected from the dispersive nature of the a_0 mode, where lower frequencies travel at lower velocities, and hence are radiated at larger values of θ from (2). Note that the air-coupled devices would be more sensitive to asymmetric mode signals in any case, as they have a greater component of out-of-plane motion than the symmetric modes, and hence couple energy more efficiently to air.

D. Waveforms in Fiber Reinforced Composites

Through-thickness and Lamb waveforms were also recorded in plates of fiber-reinforced polymer composite using the laser source and the damped lower frequency air-coupled devices. As an example, Fig. 12(a) shows a waveform for a 5.5 mm thick (40-ply) sample of cross-ply carbon fiber

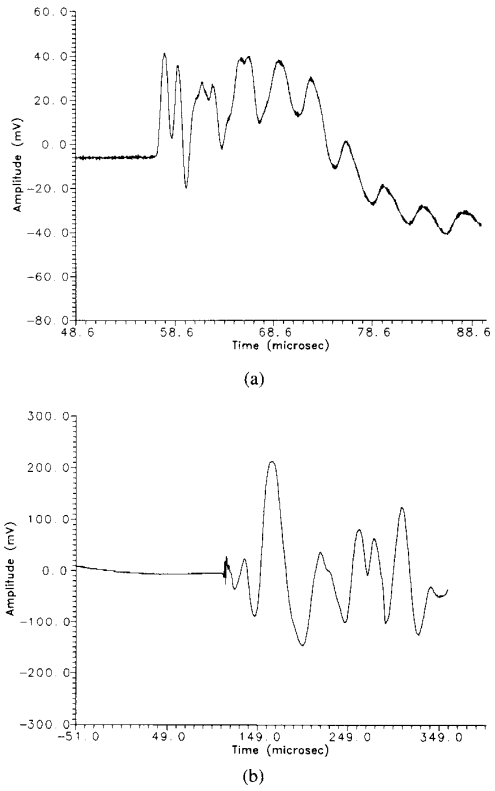

Fig. 12. Waveforms in cross-ply carbon-fiber composite plates. (a) is a through thickness waveform in a 5.5 mm 40-ply plate, and (b) a Lamb wave in a1 mm 8-ply plate, with the transducer at an angle of 12°.

composite, with a detector distance from the sample of 20 mm. Multiple longitudinal reflections are clearly visible, with a time separation of 3.6 μs. Note that the slower longitudinal velocity in this material (3000 ms^{-1}) helps visibility of the separate multiple reflections. In addition, the acoustic impedance of these materials is closer to air, increasing detection sensitivity. Lamb waves were also recorded in a 1 mm thick, 8-ply sample of the same material, and as in the case of aluminium the waveforms were a function of the receiver orientation. An example is shown in Fig. 12(b) at $\theta = 12°$. The s_0 mode could be seen at low values of θ, and decreased in magnitude as this angle was increased. However, at the same time the a_0 mode signal increased with larger values of θ until at the angle 12° shown it was a very prominent feature. The exact nature of this waveform is interesting and merits further investigation.

IV. Discussion and Conclusion

It has been demonstrated that a pulsed laser source can be used in conjunction with an air-coupled piezoelectric detector to give a completely noncontact ultrasonic transduction system. This can be used for longitudinal and shear bulk modes, Rayleigh waves, and various types of Lamb waves. The air-coupled devices have been shown to give a reasonable sensitivity to each of these modes. For bulk waves, transmission across the sample/air interface is required, and despite the fact that a low transmission coefficient exists [(1)], the transmitted signal levels were sufficient. Attenuation in air is also significant at this frequency, and this would reduce amplitudes further. Rayleigh and Lamb waves relied on the leaky nature of these modes for detection, and it was shown, as expected, that the nature of the received signal depended upon the angle θ at which the detector was placed relative to the surface, a given θ selecting a certain wave velocity. This was seen to be important in the a_0 Lamb mode in particular, due to its dispersive nature.

The capacitance device showed the types of displacements that the sample surfaces were experiencing following generation by the pulsed laser. In general, the result was a broad bandwidth transient, whereas the received signal from the air-coupled devices was dominated by their own response. It was shown in the above how this could be treated using deconvolution techniques, to separate multiple reflections.

Further work is presently being performed towards increasing and quantifying the sensitivity of detection of laser-generated transients, and to investigate configurations useful for imaging and other applications in nondestructive evaluation. These results will be presented in due course.

References

[1] D. A. Hutchins, "Ultrasonic generation by pulsed lasers," in *Physical Acoustics—Principles and Methods*, W. P. Mason and R. N. Thurston, Eds. New York: Academic, 1988, vol. XVIII, pp. 21–123.
[2] C. B. Scruby and L. E. Drain, *Laser ultrasonics: Techniques and applications*. Bristol: Adam Hilger, 1990.
[3] G. S. Taylor, D. A. Hutchins, C. Edwards, and S. B. Palmer, "TEA-CO_2 laser generation of ultrasound in non-metals," *Ultrasonics*, vol. 28, pp. 343–349, 1990.
[4] J.-P. Monchalin, "Optical detection of ultrasound," *IEEE Trans. Ultrason., Ferroelect., Freq. Contr.*, vol. 33, pp. 485–499, 1986.
[5] J. W. Wagner, "Optical detection of ultrasound," in *Physical Acoustics—Principles and Methods*, W. P. Mason and R. N. Thurston, Eds. New York: Academic, 1990, vol. XIX, pp. 201–266
[6] J.-P. Monchalin, J.-D. Aussel, P. Bouchard, and R. Heon, "Laser-ultrasonics for industrial applications," in *Review of Progress in Quantitative NDE*, D. O. Thompson and D. E. Chimenti, Eds. New York: Plenum, 1988, vol. 7B, pp. 1607–1614.
[7] W. Sachse and N. N. Hsu, "Ultrasonic transducers for materials testing and their characterisation," in *Physical Acoustics—Principles and Methods*, W. P. Mason and R. N. Thurston, Eds. New York: Academic, 1979, vol. XIV, pp. 277–406.
[8] D. A. Hutchins and J. D. Macphail, "A new design of capacitance transducer for ultrasonic displacement detection," *J. Phys. E, 18*, pp. 69–73, 1985.
[9] H. M. Frost, "Electromagnetic-Ultrasound Transducers: Principles, Practice and Applications," in *Physical Acoustics—Principles and Methods*, W. P. Mason and R. N. Thurston, Eds. New York: Academic, 1979, vol. XIV, pp. 179–275.
[10] R. B. Thompson, "Physical principles of measurements with EMAT transducers," in *Physical Acoustics— Principles and Methods*, R. N. Thurston and A. D. Pierce, Eds. New York: Academic, 1990, vol. XIX, pp. 157–199.
[11] W. Kuhl, G. R. Schodder, and F.-K. Schröder, "Condenser transmitters and microphones with solid dielectric for airborne ultrasonics," *Acoustics* , vol. 4, pp. 519–532, 1954.
[12] H. Carr and C. Wykes, "Diagnostic measurements in capacitive transducers," *Ultrasonics*, vol. 31, pp. 13–20, 1993.
[13] T. Yano, M. Tone, and A. Fukumoto, "Range finding and surface characterisation using high frequency air transducers," *IEEE Trans. Ultrason., Ferroelect. Freq. Contr.* vol. 34, no. 2, pp. 232–236, 1987.
[14] M. Babic, "A 200 kHz ultrasonic transducer coupled to the air with a radiating membrane," *IEEE Trans. Ultrason., Ferroelect., Freq. Contr.*, vol. 38, no. 3, pp. 252–255, 1991.

[15] J. A. Hossack and G. Hayward, "Finite-element analysis of 1–3 composite transducers," *IEEE Trans. Ultrason., Ferroelect., Freq. Contr.*, vol. 38, pp. 618–629, 1991.
[16] W. A. Smith and B. A. Auld, "Modelling 1–3 composite piezoelectric: Thickness-mode oscillations," *IEEE Trans. Ultrason., Ferroelect., Freq. Contr.*, vol. 38, no. 1, pp. 40–47, 1990.
[17] G. Hayward, A. Gachagan, R. Hamilton, D. A. Hutchins, and W. M. D. Wright, "Ceramic-epoxy composite transducers for non-contacting ultrasonic applications," *SPIE Symp. 1992*, vol. 1733, pp. 49–56, 1992.
[18] B. Widrow and S. D. Stearns, *Adaptive Signal Processing*. Englewood Cliffs, NJ: Prentice Hall, 1985.
[19] G. Hayward and J. Lewis, "Comparison of some non-adaptive deconvolution techniques for resolution enhancement of ultrasonic data," *Ultrasonics*, vol. 27, pp. 155–164, 1989.
[20] R. A. Wiggins, "Minimum entropy deconvolution (MED)," *Geoexploration* , vol. 16, no. 1, pp. 21–3515, 1978.

David A. Hutchins received the B.Sc. and Ph.D. degrees in 1975 and 1978, respectively.

He then worked as a post-Doctoral researcher in Denmark, England, and Canada, before becoming an Assistant Professor with the Physics Department, Queens University, Canada, in 1982. He was promoted to Associate Professor in 1985, and in 1988 moved to the Department of Engineering, University of Warwick, England, where he is a Reader. His current research interests include ultrasonic transducers, imaging, and applications in materials evaluation.

William M. D. Wright received the B.Eng. Honours degree in 1991 in mechanical engineering from the University of Warwick, England.

He is currently employed as a Research Associate in the Department of Engineering. He is also studying part time for the Ph.D. degree. His research interests include laser ultrasound, air-coupled transducers and materials characterization.

Gordon Hayward (SM'93) for a photograph and biography, see p. 578 of the September 1994 issue of this TRANSACTIONS.

Anthony Gachagan was born in Glasgow, Scotland in 1964. He received the B.Sc. Honours degree in electronic and microprocessor engineering from the University of Strathclyde in 1985.

Following his initial graduation, he worked for three years in the design and development of marine navigation equipment for S.G. Brown, Welwyn Garden City, Herts, a small subsidiary of Hawker Siddley. After which, he spent one year working for Oxford Sonicaid, Chichester, W. Sussex, on the design and development of foetal heart monitors. This was followed by two years with Tiger Communications Ltd., Marlow, Bucks, where he was employed as a software engineer developing communications products. He is currently employed as a Research Assistant at the University of Strathclyde. His research interest is in the design and evaluation of wideband transducers for through air transmission for ultrasonic nondestructive testing of polymeric fiber reinforced composite materials, as found in the aerospace industry.